

BONDING OF CERAMICS: AN ANALYSIS OF THE TORSION HOURGLASS SPECIMEN

*Original*

BONDING OF CERAMICS: AN ANALYSIS OF THE TORSION HOURGLASS SPECIMEN / Goglio, Luca; Ferraris, Monica. - In: INTERNATIONAL JOURNAL OF ADHESION AND ADHESIVES. - ISSN 0143-7496. - STAMPA. - 70:(2016), pp. 46-52. [10.1016/j.ijadhadh.2016.05.006]

*Availability:*

This version is available at: 11583/2666394 since: 2017-03-03T15:56:13Z

*Publisher:*

Elsevier

*Published*

DOI:10.1016/j.ijadhadh.2016.05.006

*Terms of use:*

This article is made available under terms and conditions as specified in the corresponding bibliographic description in the repository

*Publisher copyright*

(Article begins on next page)

BONDING OF CERAMICS: AN ANALYSIS OF  
THE TORSION HOURGLASS SPECIMEN

L. Goglio, M. Ferraris



PII: S0143-7496(16)30105-1  
DOI: <http://dx.doi.org/10.1016/j.ijadhadh.2016.05.006>  
Reference: JAAD1849

To appear in: *International Journal of Adhesion and Adhesives*

Received date: 23 February 2016

Accepted date: 16 May 2016

Cite this article as: L. Goglio and M. Ferraris, BONDING OF CERAMICS: AN ANALYSIS OF THE TORSION HOURGLASS SPECIMEN, *International Journal of Adhesion and Adhesives*, <http://dx.doi.org/10.1016/j.ijadhadh.2016.05.006>

This is a PDF file of an unedited manuscript that has been accepted for publication. As a service to our customers we are providing this early version of the manuscript. The manuscript will undergo copyediting, typesetting, and review of the resulting galley proof before it is published in its final citable form. Please note that during the production process errors may be discovered which could affect the content, and all legal disclaimers that apply to the journal pertain.

BONDING OF CERAMICS: AN ANALYSIS OF THE  
TORSION HOURGLASS SPECIMENL. Goglio<sup>#1</sup>, M. Ferraris<sup>2</sup>

<sup>1</sup> Department of Mechanical and Aerospace Engineering - DIMEAS, Politecnico di Torino,  
corso Duca degli Abruzzi 24, Torino, 10129, Italy

<sup>2</sup> Department of Applied Science and Technology - DISAT, Politecnico di Torino,  
corso Duca degli Abruzzi 24, Torino, 10129, Italy

## Abstract

There is a recent and growing interest in joining ceramic parts due to their increased use in several fields such as next-generation nuclear plants, aeronautic engine parts and aerospace components. For high temperature applications, glass-ceramics are used as an “adhesive” for ceramic parts, this generates the need for test methods suitable to assess their bond strength. Unfortunately, the various test procedures currently used lead to different results.

One recent test is based on torsion of hourglass shaped joined ceramics, originated from a modification of the ASTM F734-95 standard, with the aim of obtaining failure under a pure shear state in the bondline subjected to torsion.

However, results obtained from different versions of the hourglass geometry show differences which are still difficult to compare. Moreover, due to the brittle nature of the materials and especially when the adhesive strength is comparable to that of the substrates, the failure is not confined in the bond and propagates also in the substrates. In this case, the results are still of arguable application for design purposes.

The aim of this paper is to give an insight on torsion of hourglass-shaped joined ceramics and on the interpretation of the obtained results, by means of detailed analytical and numerical studies of the stress distribution in the specimen, and taking into account the brittle nature of

---

<sup>#</sup> Corresponding author. Tel. +39 011 0906934; email [luca.goglio@polito.it](mailto:luca.goglio@polito.it) (L. Goglio)

the materials. The main findings are: i) the stress state in the bondline is not singular; ii) a non negligible stress concentration arises out of the bondline.

Keywords A: High temperature adhesives; B: Ceramics, glass; C: Finite element stress analysis, joint design; Torsion test.

Accepted manuscript

## 1. Introduction

Ceramics can offer several advantages in terms of strength and hardness, especially under harsh conditions, that exceed the resistance of metals. Low induced radioactivity, thermal stability and resistance to irradiation, in addition to mechanical strength, make SiC-based ceramics suitable for nuclear applications, especially for fusion reactors, and a wide amount of related studies has been presented since long (e.g. [1]-[5]). Moreover, recently developed aeronautic and aerospace engines use SiC-based composites to improve high temperature resistance in several engine parts [6].

The use of ceramics as a structural material originates the need for suitable joining techniques; being impossible to use welding, several ad hoc solutions have been proposed, most of them based on hot pressing techniques [4],[5]. To avoid the need for pressure, glass ceramics are used as pressure-less high temperature resistant joining materials for SiC based components [7]. In turn, joining originates the need for a suitable test method to assess the mechanical strength of the joints, and the most significant parameter is deemed to be the shear strength expressed as stress corresponding to the failure load [7],[8].

To this aim, several test methods and specimen types were investigated in the last years. The preferred method to measure the strength of bonded ceramics should be the four-point asymmetrical (i.e. antisymmetric) bending test, ASTM C1469 standard [9]. A wide comparison among results obtainable from ASTM C1469 and several other test methods was carried out as an international cooperation ([10]-[12]). At that stage, to speed up the preparation of the specimens, epoxy adhesive Araldite AV119 (Huntsman Advanced Materials, Basel, Switzerland) was used as a “model” bonding material, suitable to investigate the response of the different specimen types, although the quantitative results were not of interest for high temperature applications.

Lap joint specimens for ceramics of various types (single- or double-lap offset in compression, double-notch in compression [10]) have the common shortcoming of creating in the bond a mix of normal and shear stresses, both non-constant, thus the obtained result is only an apparent shear strength.

Regarding the four-points asymmetrical test ASTM C1469 [9], which should ideally create only shear stress in the bond, several problems associated with it were pointed out [10], due to: i) the influence of even small misalignments of the specimen and the loading pins; ii) the need for machining notches in the joint if the bonding material strength is in the range 25%-50% of the base material strength and the impossibility of applying the method if the bonding material strength exceeds 50% of the base material strength; iii) the difficulty in manufacturing the specimens by cutting from a wider block or preparing them one by one. Moreover, surprisingly, such standard evaluates the shear strength simply as shear force to area ratio, neglecting that the peak stress in the section (parabolic distribution) is 1.5 times higher.

Torsion, causing a state of shear stress in the specimen cross section, is the most promising testing condition. However, in case of square section also normal stress is induced by constrained section warpage in the fixtures; indeed, failures occurred in the SiC, out of the bond [11]. Conversely, torsion of a circular section causes a state of pure shear stress in the specimen, as needed. Unfortunately, results from simple cylindrical specimen exhibited a large scatter, likely due to surface defects; this evidenced the need for creating the bond in a reduced section, designed as the “weakest ring” of the system where failure must occur. Moreover, a straight cylindrical bar requires tight clamping of the ends to apply the torque, which can cause local failure.

Accounting for these issues, the hourglass specimen shown in Fig. 1 was cooperatively

proposed by Oak Ridge National Laboratory (USA), Kyoto University (Japan) and Politecnico di Torino (Italy) by modifying the specimen foreseen in the ASTM F734-95 standard [13]. It has the merit to generate a pure shear stress condition in the bond section, while the increased area in the remainder of the specimen makes a failure due to local defects less likely. Moreover, thanks to the square section of the ends, the torque can be applied easily. The size was chosen very small (bonded section diameter 5 or 4 mm) to obtain miniature specimens, easy to be placed in the limited available space when they were exposed to irradiation for nuclear studies [14].

Obviously, the shear stress distribution in a section subjected to torsion is not constant, but can be simply calculated with the well known formula

$$\tau = \frac{T}{J} x \quad (1)$$

where T is the torque, J is the sectional polar moment of inertia and x is the radial coordinate. Eq. (1) does not account for the notch effect due to the non-straight profile of the specimen, which however can be included multiplying by the relevant stress concentration factor  $K_t$ .

This type of geometry was used with encouraging results in several test campaigns, for both AV119-bonded [11],[12] and calcia-alumina glass-ceramic (CA)-bonded [15],[16] specimens.

In the case of AV119-bonded specimens the adhesive strength, calculated by substituting in eq. (1) the ultimate value of T, resulted dependent on the size of the specimen [12]. The reason is that such adhesive is to a certain extent ductile; upon loading, once the yield stress is reached in the outer radius, plasticity spreads inwards and the torque can increase, thus the ultimate torque value is attained when the whole section is yielded and depends on section size. Obviously, under such conditions, eq. (1) is no longer appropriate.

In the case of CA-bonded specimens, it was noticed that in several instances the failure affects

the adherends bulk and not only the bond [15]. It was argued if the results obtained under these conditions are comparable to those obtained when the failure affects only the bond.

Trying to address these issues, modified versions of the hourglass specimen geometry were tested, in particular by creating a hollow bonded section (internal diameter 3 mm), obtained either by drilling full half-specimens or by machining half-specimens with ring-shaped section, then bonding them [15],[16].

In the case of ductile adhesive, the hollow geometry approximates the ideal situation of a thin ring, in which all the adhesive is at the same distance from the section centre so that the progressive (from outer radius inwards) yielding is avoided.

In the case of brittle glass-ceramic adhesive (CA), it was expected that the hollow geometry could “constrain” the failure to occur only in the bond, without affecting the SiC. The latter fact was checked experimentally in [16] (selected data reported in Table 1 for convenience); it was found that also for the hollow specimens, even more frequently than for the full specimens, the fracture affected the SiC. More specifically, it was observed that the fracture could even start in the SiC, then propagate in the CA. The strength measured from hollow specimens (last two lines in Table 1) was generally lower.

Strength data in Table 1 are simply obtained by applying eq. (1), thus the stress concentration effect is not accounted for. In a broader view, a more sophisticated assessment of the stress state in the joint specimen would be advisable.

Therefore, a theoretical -analytical and numerical- investigation on the specimen properties can be useful to explain its behaviour. The present paper reports the outcome of a study carried out with this aim. First, the relevant mathematical aspects of the stress state in the specimens are considered; then, the numerical modelling and the obtained outputs are described; finally, the results are used to propose an explanation of the experimentally



observed behaviour.

## 2. Hourglass specimen: theoretical aspects

The specimen presents the typical features of a bi-material interface (Fig. 2a); the most important aspect is the possible singularity of the elastic stresses in the interface end. It is worth noting that, since both materials involved (SiC and CA glass-ceramic) are brittle, their stress-strain relationship is practically linear, thus an elastic solution can be significant to predict failure.

The problem is ruled by the angles of the materials in the interface end and by their elastic constants. Although the loading condition of actual interest, i.e. torsion, is non-planar, for the sake of completeness and comparison also the in-plane behaviour is considered first. From the practical viewpoint, this can be useful to predict the response of the specimen if loaded accidentally (e.g. due to a misalignment in the test rig) in tension. The case, well known in the literature, is described by the Bogy determinant [17] (see also [18] for an application to ceramics), which, in turn, depends on the Dundurs constants  $\alpha$ ,  $\beta$  [19] and on the angles  $\gamma_1$ ,  $\gamma_2$ . The values of the auxiliary parameter  $p$ , which make the determinant  $D$  vanish, control the singularity conditions of the generic stress component  $\sigma_{ij}$ :

$$D(\gamma_1, \gamma_2, \alpha, \beta; p) = 0 \quad (2)$$

$$\sigma_{ij}(r, \theta) \propto r^\lambda f_{ij}(\theta) + \dots \quad (3)$$

where  $f_{ij}(\theta)$  is an angular function and  $\lambda = p - 1$ , thus  $\sigma_{ij}$  is singular if  $p$  (its real part, if complex) lies in the interval  $]0, 1[$ . Strictly speaking, the Bogy's theory applies to a planar case; however, as will be seen in the next section, the comparison with the numerical results shows that the approach is applicable with good approximation to the axi-symmetric case under examination. Assuming the data reported in Table 2 and plane strain condition for the

calculation of  $\alpha$  and  $\beta$ , it results  $\lambda = -0.079$ , so the stress field is moderately singular.

Considering now the torsional behaviour, this problem received less attention in the literature; however, two different relevant published studies are suitable. Ma and Hour [21] applied the Mellin transform to the equilibrium equation written in terms of the hoop displacement  $w$

$$\frac{\partial^2 w}{\partial r^2} + \frac{1}{r} \frac{\partial w}{\partial r} + \frac{1}{r^2} \frac{\partial^2 w}{\partial \theta^2} = 0 \quad (4)$$

obtaining for the transformed displacement  $\hat{w}$  the solution

$$\hat{w}(s, \theta) = a(s) \sin(s\theta) + b(s) \cos(s\theta) \quad (5)$$

where  $s$  is the transform parameter and  $a(s)$ ,  $b(s)$  are functions to be determined from the boundary conditions (the relevant one is the applied displacement at the unbonded boundary faces).

A different approach to the same problem was used by Qian and Hasebe [22] who, using the eigenfunction expansion method, wrote for each material ( $i = 1, 2$ ) the solution of eq. (4) in the form  $w_i(r, \theta) = r^\lambda F_i(\theta, \lambda)$ , where  $F_i$  is an unknown function and  $\lambda$  has a slightly different meaning compared to eq. (3) (i.e. it is the exponent in the displacement formula instead of the stress formula), obtaining:

$$w_i(r, \theta) = r^\lambda [A_i \cos(\lambda\theta) + B_i \sin(\lambda\theta)] \quad (6)$$

where  $A_i$  and  $B_i$  are constants determined from the boundary conditions.

Both approaches [21],[22] lead to the same eigenequation, which in a unified notation can be written

$$G_1 \sin(\lambda\gamma_1) \cos(\lambda\gamma_2) + G_2 \sin(\lambda\gamma_2) \cos(\lambda\gamma_1) = 0 \quad (7)$$

where  $G_1$  and  $G_2$  are the shear moduli of the two materials. It results that the stresses  $\tau_{zr}$ ,  $\tau_{z\theta}$

are singular if there is a root  $\lambda$  (eigenvalue) of eq. (7) in the interval  $]0,1[$ . By assuming the data of Table 2 this is not verified, thus the stress field in the bond of the hourglass specimen subjected to torsion is non-singular. This fact is strictly related to the angles at the interface: in the ideal geometry, at the bondline, both the tangent to the rounded adherend side and the straight side of the adhesive are parallel to the specimen axis, thus  $\gamma_1 = \gamma_2 = 90^\circ$  (Fig. 2b). Any deviation from this condition on the profile would cause stress singularity.

### 3. Hourglass specimen: finite element modelling

The analytical approaches reported above applies to the description of the stress field in the neighbourhood of the bi-material interface end, but clearly cannot yield the stress field in the whole specimen. Moreover, whilst the singularity can be assessed analytically, the intensity of the stress field (namely the stress intensity factor) needs to be calculated numerically [23].

A finite element (FE) model of the specimen was built and solved with the Ansys® code [24], considering, for the sake of completeness, both cases of tension and torsion. As the mesh had to be extremely refined near the interface to account for the singularity, a two-dimensional axisymmetric model was adopted. Indeed, it was deemed that the deviation from axial symmetry in the square ends of the specimen did not affect its central portion. Taking advantage of the symmetry with respect to the mid-thickness plane of the CA glass-ceramic layer, only the upper half-specimen was modelled. Figure 3 shows an overall view of the mesh and details of the bond.

The same discretization was used for tension and torsion, the element type was the SOLID273, eight-noded continuum axisymmetric including hoop displacement to account for the torsional behaviour. The overall element size along the SiC-CA interface was  $5 \cdot 10^{-3}$  mm, reduced to  $2 \cdot 10^{-5}$  mm in the neighbourhood of the potentially singular point. Such a small size also far from the singularity was dictated by the need for having a sufficient number of

elements (eight) in the CA half layer, which is about 0.04 mm thick. Convergence check was carried out on the stress distribution in the mid-thickness of the joint (obviously, convergence on the peak values related to the singularity is intrinsically impossible). The model consisted of 141413 nodes and 46896 elements for the non-hollow specimen, 125570 nodes and 41705 elements for the hollow specimen. The loading conditions were simulated (Fig. 3) by prescribing an axial displacement of the end section in case of tension, and a hoop displacement of the cylindrical side in case of torsion. All calculations required about one minute CPU time each on an intel i5® CPU computer.

#### 4. FE results (linear elastic analysis)

##### 4.1. Tension

The loading condition was defined to create a “nominal” tensile stress in the bond of 10 MPa (calculated as force to area ratio). In the mid-thickness plane of the CA, as shown in Fig. 4a, the stress distribution is non-singular and similar to the case of a notched bar. The axial stress is prevalent and exhibits a maximum near the outer radius (note that in case of a single material the peak would be exactly at the outer radius), the stress concentration factor is  $K_t = 1.73$ . The hoop and radial stresses have smaller values and similar distributions, except for the outer radius where the radial stress must vanish.

In the SiC-CA interface, Fig. 4b, the FE results substantially confirm the theoretical prediction given by the Bogy determinant [17]. The stress field is singular, the local fitting of the results yields for the exponent  $\lambda$  values equal to -0.071 and -0.073 respectively for the axial and hoop stresses, thus very close to the analytical prediction reported above -0.079 (different values, -0.058 and -0.054 are respectively obtained by fitting the radial and shear stresses, which have lower values thus the interpolation is less accurate).

#### 4.2. Torsion

Torsion is the actual condition of test for which the hourglass specimen is designed and intended to be used. In this case the loading condition was defined to create a peak “nominal” shear stress in the bond of 10 MPa (value calculated by means of eq. (1) equalling  $\tau$  to the radius of the bond, 2.5 or 2 mm).

Considering first the non-hollow specimen, in the mid-thickness plane of the CA (Fig. 5a) the shear stress distribution is not singular and slightly non-linear; the peak is situated at the outer radius and value of the stress concentration factor  $K_t$  is 1.29 or 1.21 respectively for bond diameter 5 or 4 mm. The other stress components, in particular the normal axial, are nil, thus a pure state of torsion is created in the mid-thickness plane. In the SiC-CA interface, as shown in Fig. 5b, the FE results confirm the theoretical prediction given by the Ma and Hour [21] or Qian and Hasebe [22] theories leading to eq. (7): the practically flat regression line (slope, i.e. singularity exponent,  $\lambda=-0.003$ ) indicates that the stress field is non-singular. Figure 6a shows the contour plot of the major principal stress in the whole hourglass specimen with bond diameter 5 mm; it is interesting to notice that the most stressed zone (maximum value about 15 MPa) is in the filleted edge at a distance from the SiC-CA interface, as shown in detail by Fig. 6b). The plot corresponding to bond diameter 4 mm is equivalent and not shown for brevity.

Similar results were found for the hollow specimen. In the mid-thickness plane of the CA (Fig. 7) the stress distribution is again not singular and slightly non-linear, with peak at the outer radius and stress concentration factor  $K_t = 1.37$ . The contour plot of the major principal stress (Fig. 8) shows again that the most stressed zone occurs in the SiC along the filleted edge, at a distance from the interface. All values are somewhat higher than in the case of non-hollow specimen.

## 5. Discussion

The obtained results add useful insight on the features of the hourglass specimen.

A first important point is that, under torsion, the stress state in the bond cross-section is of pure shear, differently from all lap test geometries (which exhibit a mix of shear and peel components); moreover, in spite of the presence of a bi-material interface, no singular behaviour of the stresses occurs. The analytical treatment leading to eq. (7) and the numerical results (fitting in Fig. 5b) confirm reciprocally this result. This is clearly a merit of the hourglass geometry. On the other hand, the analysis showed that the hourglass geometry leads to a stress singularity in case of tensile loading, which is not the relevant testing condition but could be unintentionally applied due to misalignments of the testing set (incidentally, it can be remarked that the Bogy theory, although formulated for plane stress/strain conditions, gives a satisfactory prediction also in this axisymmetric case). Care must be taken in this sense during the experiments.

A second point is that the hourglass geometry causes a moderate but non negligible stress concentration factor,  $K_t = 1.29, 1.21, 1.37$  as respectively found in the different considered cases. Thus, the mere application of eq. (1) is not sufficient, the relevant  $K_t$  values must be applied to the data of Table 1 to make the results comparable in terms of true stress at fracture. At the same time, the statistical scatter of the results must be accounted for. Classical t and F test can be applied to analyse the data as follows:

- 1) Considering first the full specimens, the values of strength obtained from  $D=5$  mm and  $D=4$  mm must be compared separately in the cases of fracture in CA only or in CA and SiC.
  - a) In case of fracture in CA only, the related statistical values are  $F=3.157$ ,  $F_{0.95}=224.6$  (0.95 confidence level) and  $t=0.475$ ,  $t_{0.95}=2.571$ ; thus the data can be assumed as

coming from the same distribution, with mean 131.4 MPa and standard deviation 24.0 MPa (units are omitted in the following for brevity); here and in all following similar steps the pooled mean and standard deviation are obtained as weighed values, accounting for the numbers of specimens of each case (see Appendix).

- b) Similarly, in case of fracture affecting CA and SiC, the related statistical values are  $F = 3.481$ ,  $F_{0.95} = 234.0$  and  $t = 0.207$ ,  $t_{0.95} = 2.365$ ; again, the data can be assumed as coming from the same distribution with mean 146.7 and standard deviation 25.7.
  - c) Comparing the two types of fracture (CA, CA and SiC) for  $D=5$  mm and  $D=4$  mm pooled together, the related statistical values are  $F = 1.147$ ,  $F_{0.95} = 4.147$  and  $t = 1.215$ ,  $t_{0.95} = 2.145$ ; thus, the data can be assumed as coming from the same distribution, with mean 140.0 and standard deviation 25.0.
- 2) Considering next the hollow specimens, no case of fracture in CA only is available from drilled specimens and the values from ring-shaped specimens are so low that any statistical consideration is superfluous; regarding the case of fracture affecting CA and SiC, the related statistical values are  $F = 1.960$ ,  $F_{0.95} = 3.230$  and  $t = 1.325$ ,  $t_{0.95} = 2.110$ ; thus, the data can be assumed as coming from the same distribution, with mean 114.0 and standard deviation 24.8.
  - 3) Finally, the data obtained from full and hollow specimens (of both diameters) are compared; the related statistical values are  $F = 1.016$ ,  $F_{0.95} = 2.353$  and  $t = 3.088$ ,  $t_{0.95} = 2.035$ , so the two means are significantly different.

Therefore it comes out that, having taken into account the related stress concentration factors for a fair comparison, the use of hollow specimens yields an unduly lower strength value. This outcome can be most likely ascribed to uncontrollable defects created by machining or joining of such a small ring shaped area.

An open issue regarding this testing activity is the search for a “pure” shear strength, believed to be significant only if the fracture occurs in the cross-sectional plane of the specimen. The underlying problem is that, although the shear stress caused by torsion occurs in such a plane, brittle materials as CA glass-ceramic and SiC tend to fail under the action of the highest normal stress (namely the major principal stress), which notoriously acts in a plane  $45^\circ$  skew with respect to the cross-section. This justifies the cone-shaped fractures frequently observed experimentally [15].

Indeed, if the strength of a brittle joining material (CA) is low enough compared to that of the ceramic (SiC), the fracture, although initiated on a skew plane in the joining material, cannot cross the interface and is confined in the bond; thus it appears macroscopically in the cross-section. Conversely, if the strengths of the two materials are comparable, or the strength of the ceramic is lower than that of the joining material, a fracture originated in the bond can cross the interface and propagate in the ceramic, creating a cone-shaped final appearance.

It is also possible that a fracture starts in the ceramic, where FE modelling pinpoints the most stressed zone, then propagates in the bond. These findings are in accordance with the results presented by Henager et al. [25], who –although dealing with different aspects of the hourglass specimen behaviour, namely the damage accumulation due to irradiation and the elasto-plasticity in case of ductile adhesive– noticed a stress concentration in the filleted edge.

Thus a suitable improvement of the hourglass specimen should aim at reducing as much as possible the stress concentration in the filleted edge, to prevent a fracture type which is not significant to assess the strength of the bond.

## 6. Conclusions

The review of previous experimental results, based on the analytical and numerical study of



the hourglass specimen of SiC bonded by a calcia-alumina (CA) glass-ceramic carried out in this work, suggests the following conclusions:

- the hourglass specimen geometry avoids stress singularity in the bi-material interface (provided that the profile of the specimen is locally orthogonal to the interface), care must be taken in the experimental setup to avoid spurious loading (e.g. tension) which can cause singular stresses;
- a moderate but non negligible stress concentration arises, which must be taken into account to assess the strength in terms of true stress (especially for comparison of different geometries);
- the hollow configuration of the hourglass specimen is not suitable, both for the higher stress concentration that takes place and for the defects created by machining;
- as the materials under test are brittle, a non-planar fracture surface under torsion loading is unavoidable, except for the case of an adherend material much stronger than the adhesive; improvements should aim at preventing stress concentration out of the bondline.

#### Acknowledgments

The authors would thank Prof. D. Paolino (Politecnico di Torino) for the helpful discussion on the statistical treatment of the experimental results.

#### References

- [1] L.L. Snead, O. Schwartz. Advanced SiC for fusion application. J. Nucl. Mater. 219:3-14 (1995).
- [2] P. Fenici, A.J. Frias Rebelo, R.H. Jones, A. Kohyama, L.L. Snead. Current status of SiC/SiC composites R&D. J. Nucl. Mater. 258-263:215-225 (1998).
- [3] L. Giancarli, H. Golfier, S. Nishio, R. Raffray, C. Wong, R. Yamada. Progress in blanket designs using SiC<sub>f</sub>/SiC composites. Fusion Eng. Des. 61-62:307-318 (2002).

- [4] T. Nozawa, T. Hinoki, A. Hasegawa, A. Kohyama, Y. Katoh, L.L. Snead, C.H. Henager Jr., J.B.J. Hegeman. Recent advances and issues in development of silicon carbide composites for fusion applications. *J. Nucl. Mater.* 386-388: 622-627 (2009).
- [5] L.L. Snead, T. Nozawa, M. Ferraris, Y. Katoh, R. Shnavski, M. Sawan. Silicon carbide composites as fusion power reactor structural materials. *J. Nucl. Mater.* 417:330-339 (2011).
- [6] CFM LEAP-1A powers Airbus A321neo first flight. CFM Press Center, February 9 2016. <http://www.cfmaeroengines.com/press>.
- [7] M. Ferraris, M. Salvo, V. Casalegno, S. Han, Y. Katoh, H.C. Jung, T. Hinoki, A. Kohyama. Joining of SiC-based materials for nuclear energy applications. *J. Nucl. Mater.* 417:379-382 (2011).
- [8] H.C. Jung, T. Hinoki, Y. Katoh, H. Kohyama. Development of a Shear Strength Test Method for NITE-SiC Joining Material. *J. Nucl. Mater.* 417:383-386 (2011).
- [9] ASTM C1469-10. Standard test method for Shear Strength of Joints of Advanced Ceramics at Ambient Temperature. ASTM Int. (2010).
- [10] M. Ferraris, A. Ventrella, M. Salvo, M. Avalor, F. Pavia, and E. Martin. Comparison of Shear Strength Tests on AV119 Epoxy-Joined Carbon/ Carbon Composites. *Compos. Part B-Eng.* 41:182-191 (2010).
- [11] M. Ferraris, M. Salvo, V. Casalegno, A. Ventrella, M. Avalor. Torsion Tests on AV119 Epoxy-Joined SiC. *Int. J. Appl. Ceram. Technol.* 9:795-807 (2012).
- [12] M. Ferraris, A. Ventrella, M. Salvo, D. Gross. Shear strength measurements of AV119 epoxy-joined SiC by different torsion tests. *Int. J. Appl. Ceram. Technol.* 11:394-401 (2014).
- [13] ASTM F734-95, Standard Test Method for Shear Strength of Fusion Bonded Polycarbonate Aerospace Glazing Material, ASTM Int. (2011).

- [14] Y. Katoh, L.L. Snead, T. Cheng, C. Shih, W.D. Lewis, T. Koyanagi, T. Hinoki, C.H. Henager Jr., M. Ferraris. Radiation-tolerant joining technologies for silicon carbide ceramics and composites. *J. Nucl. Mater.* 448:497-511 (2014).
- [15] M. Ferraris, M. Salvo, S. Rizzo, V. Casalegno, S. Han, A. Ventrella, T. Hinoki, Y. Katoh. Torsional Shear Strength of Silicon Carbide Components Pressurelessly Joined by a Glass-Ceramic. *Int. J. Appl. Ceram. Technol.* 9:786-794 (2012).
- [16] M. Ferraris, A. Ventrella, M. Salvo, Y. Katoh, D. Gross. Torsional Shear Strength Tests for Glass-Ceramic Joined Silicon Carbide. *Int. J. Appl. Ceram. Technol.*, 12:693-699 (2015).
- [17] D. B. Bogy. Two edge-bonded elastic wedges of different materials and wedge angles under surface tractions. *J. Appl. Mech.* 38:377-86 (1971).
- [18] P. A. Kelly, D. A. Hills, D. Nowell. The design of joints between elastically dissimilar components (with special reference to ceramic/metal joints). *J. Strain Analysis* 27:15-20 (1992).
- [19] J. Dundurs. Discussion of the paper “Edge-bonded dissimilar orthogonal elastic wedges under normal and shear loading”. *J. Appl. Mech.* 36:650-652 (1969).
- [20] CVD Silicon Carbide, Rohm and Haas (2008).
- [21] C.-C. Ma, B.-L. Hour. Analysis of dissimilar anisotropic wedges subjected to antiplane shear deformation. *Int. J. Solids Structures* 25:1295-1309 (1989).
- [22] J. Qian, N. Hasebe. Property of eigenvalues and eigenfunctions for an interface V-notch in antiplane elasticity. *Eng. Fract. Mech.* 56: 729-734 (1997).
- [23] L. Goglio, M. Rossetto. Evaluation of the singular stresses in adhesive joints. *J. Adhesion Sci. Technol.* 23:1441-1457 (2009).
- [24] ANSYS release 15.0 Mechanical APDL Documentation, ANSYS Inc. (<http://www.ansys.com>), Canonsburg, PA, USA.

- [25] C.H. Henager Jr., B.N. Nguyen, R.J. Kurtz, T.J. Roosendaal, B.A. Borlaug, M. Ferraris, A. Ventrella, Y. Katoh. Modeling and testing miniature torsion specimens for SiC joining development studies for fusion. J. Nucl. Mater. 466:253-268 (2015).

## Appendix

In the statistical analysis of the data, the pooled mean  $\bar{X}_{12}$  and standard deviation  $S_{X_1X_2}$  of the two datasets under consideration are calculated as follows:

$$\bar{X}_{12} = \frac{\bar{X}_1 n_1 + \bar{X}_2 n_2}{n_1 + n_2} \quad (A1)$$

$$S_{X_1X_2} = \sqrt{\frac{(n_1 - 1)S_{X_1}^2 + (n_2 - 1)S_{X_2}^2}{n_1 + n_2 - 2}} \quad (A2)$$

where, respectively for each dataset ( $i = 1, 2$ ),  $n_i$  is the number of specimens,  $\bar{X}_i$  is the mean and  $S_i^2$  is the variance.

## LIST OF FIGURE CAPTIONS

Fig. 1. Schematic of the hourglass specimen.

Fig. 2. Bi-material interface end: a) general case; b) hourglass specimen.

Fig. 3. FE model of the hourglass specimen: a) overall view; b), c) details of the bond.

Fig. 4. FE results for the hourglass specimen ( $D = 5 \text{ mm}$ ) under tension: a) stresses in the mid-thickness plane of the CA; b) singular stress field near the SiC-CA interface corner and related power-law formulae  $\sigma = H r^\lambda$  ( $H$  stress intensity factor,  $\lambda$  singularity exponent), filled symbols show the points used for fitting.

Fig. 5. FE results for the hourglass specimen under torsion: a) shear stress in the mid-thickness plane of the CA; b) non-singular stress field near the SiC-CA interface corner and related power-law formula  $\sigma = H r^\lambda$  ( $H$  stress intensity factor,  $\lambda$  singularity exponent  $\approx 0$ ), filled symbols show the points used for fitting.

Fig. 6. Contour plot of the major principal stress in the hourglass specimen under torsion: a) overall view; b) detail of the stress concentration.

Fig. 7. FE results for the hollow hourglass specimen under torsion: shear stress in the mid-thickness plane of the CA.

Fig. 8. Contour plot of the major principal stress (MPa) in the hollow hourglass specimen under torsion: a) overall view; b) detail of the stress concentration.

## LIST OF TABLE CAPTIONS

Table. 1. Shear strength (mean  $\pm$  standard deviation) obtained from different tests on hourglass specimens by applying eq. (1); selected values from [16].

Table 2. Data relevant to interface singularity.

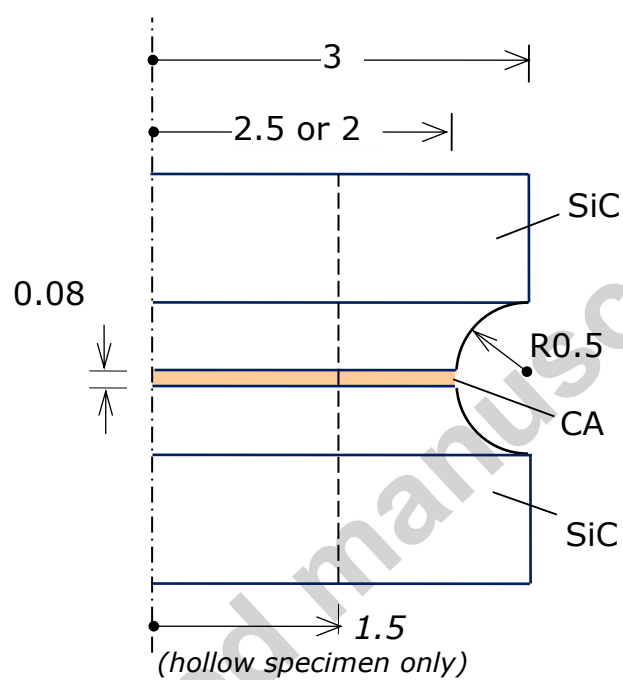


Fig. 1. Schematic of the hourglass specimen (dimensions in mm).

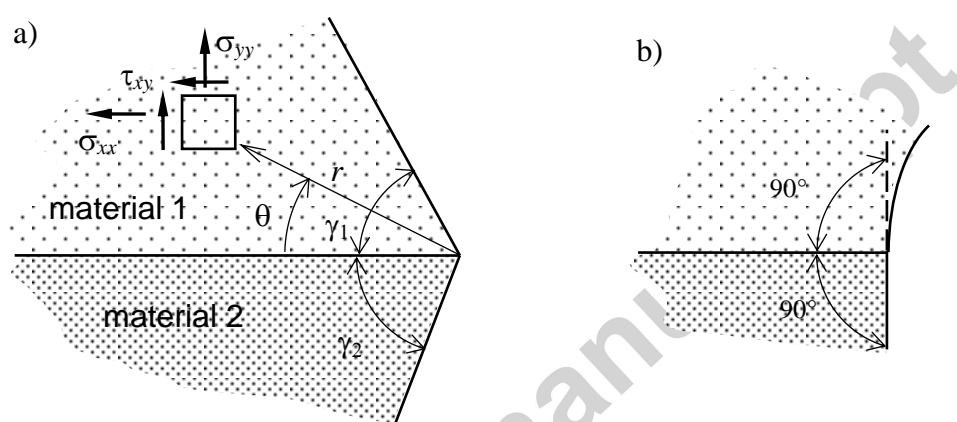


Fig. 2. Bi-material interface end: a) general case; b) hourglass specimen.



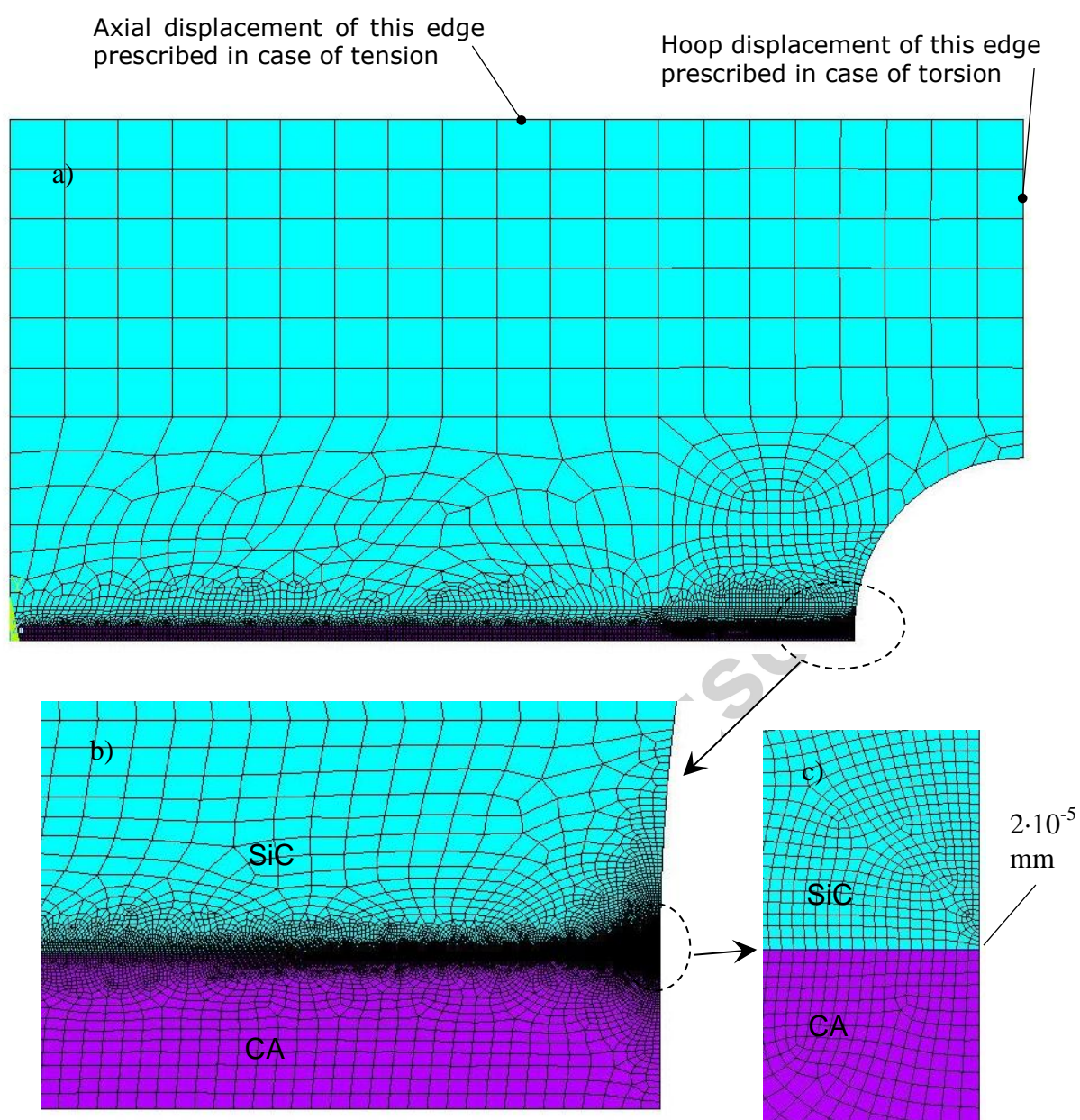


Fig. 3. FE model of the hourglass specimen: a) overall view, b) and c) details of the bond.

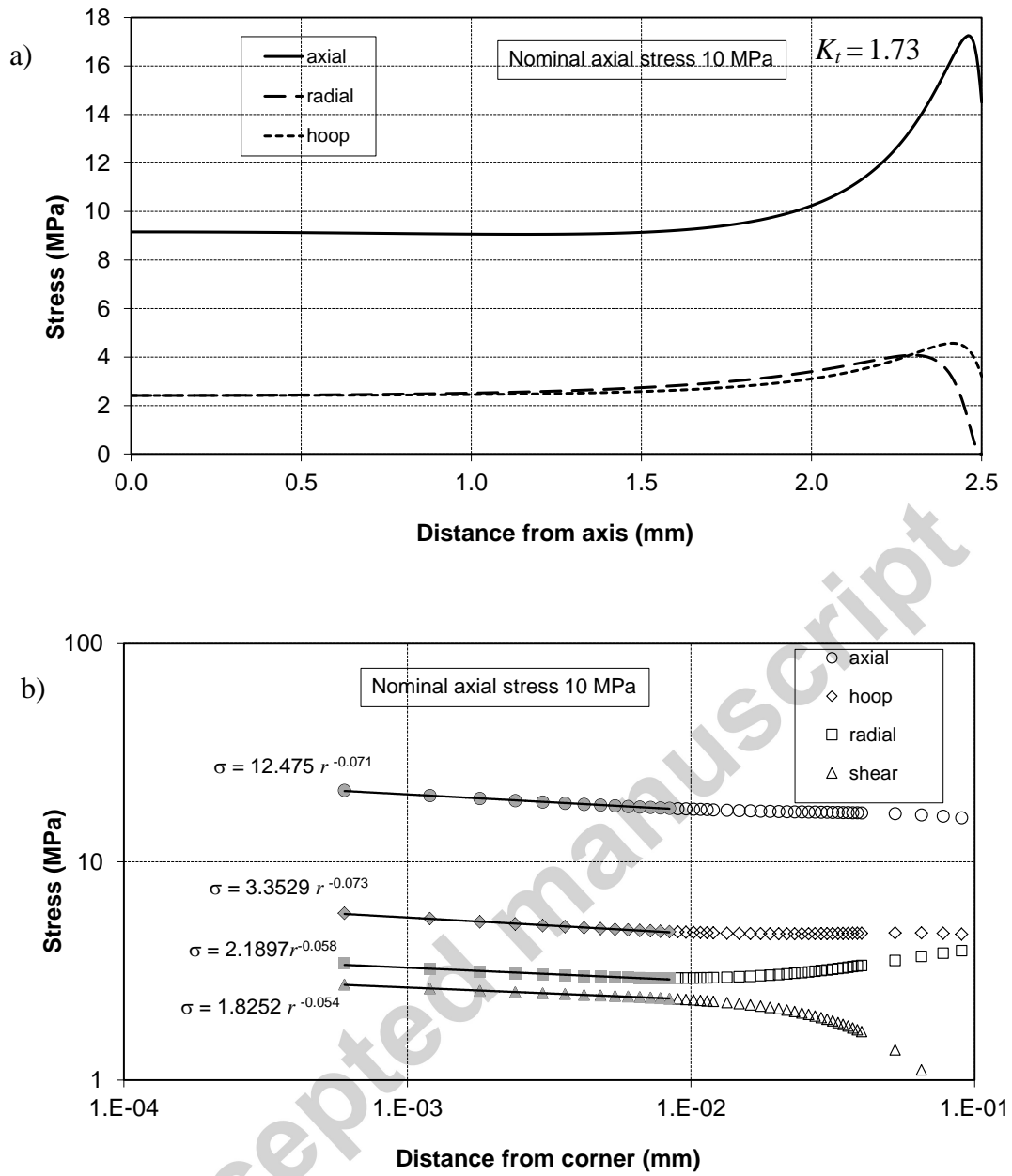


Fig. 4. FE results for the hourglass specimen (D=5 mm) under tension: a) stresses in the mid-thickness plane of the CA; b) singular stress field near the SiC-CA interface corner and related power-law formulae  $\sigma = H r^\lambda$  ( $H$  stress intensity factor,  $\lambda$  singularity exponent), filled symbols show the points used for fitting.

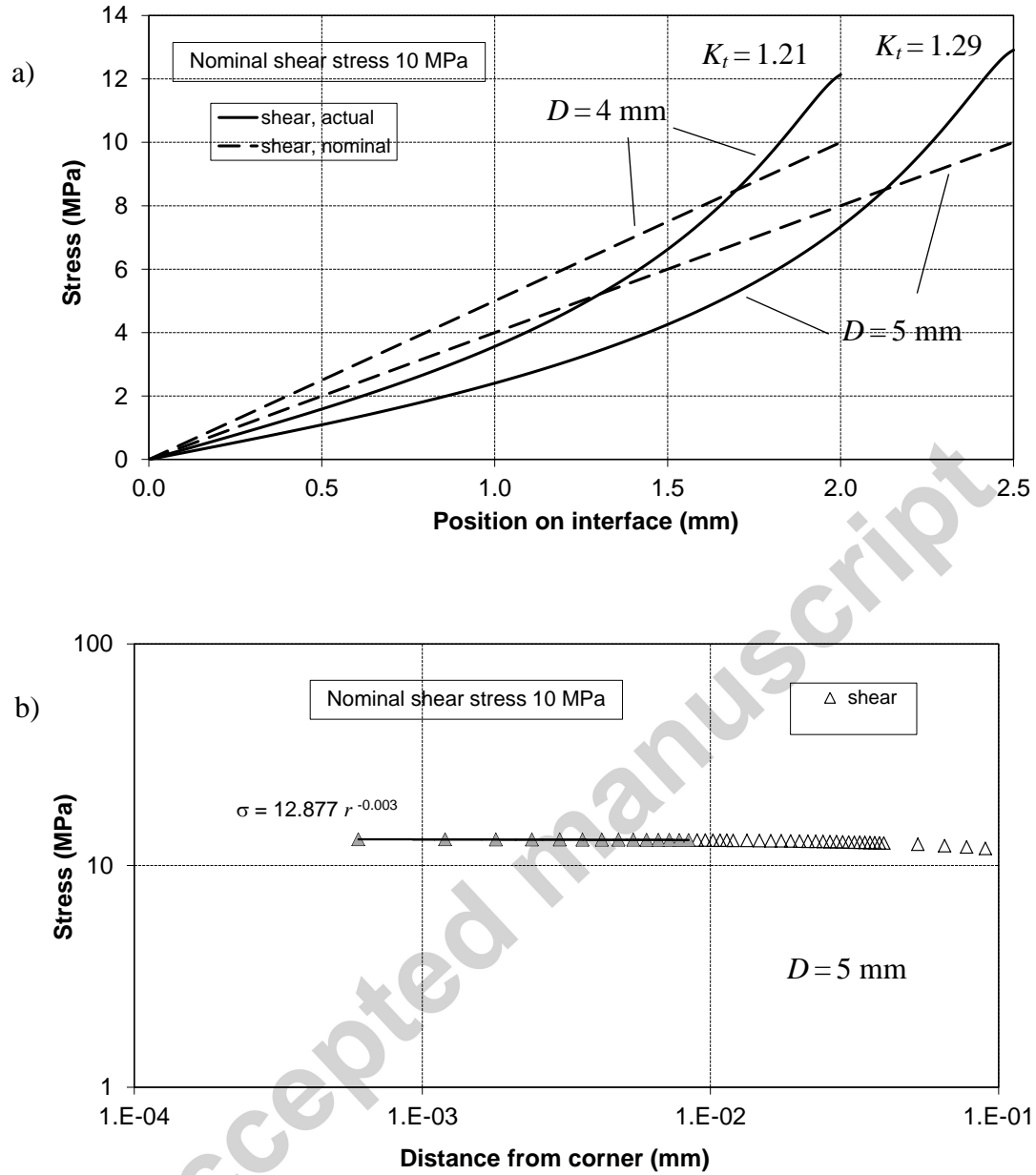


Fig. 5. FE results for the hourglass specimen under torsion: a) shear stress in the mid-thickness plane of the CA; b) non-singular stress field near the SiC-CA interface corner and related power-law formula  $\sigma = H r^\lambda$  ( $H$  stress intensity factor,  $\lambda$  singularity exponent  $\approx 0$ ), filled symbols show the points used for fitting.

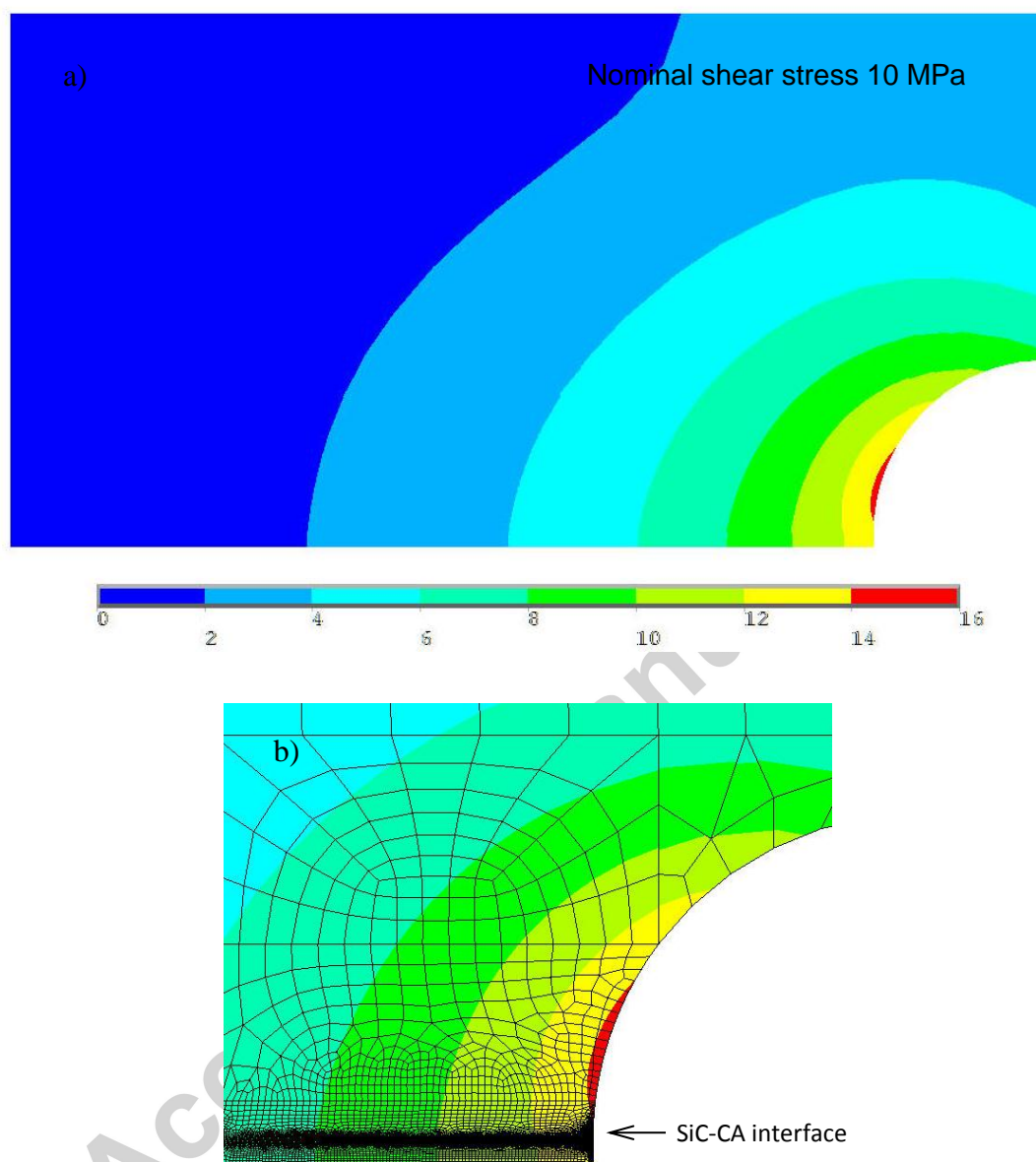


Fig. 6. Contour plot of the major principal stress (MPa) in the hourglass specimen under torsion: a) overall view; b) detail of the stress concentration.

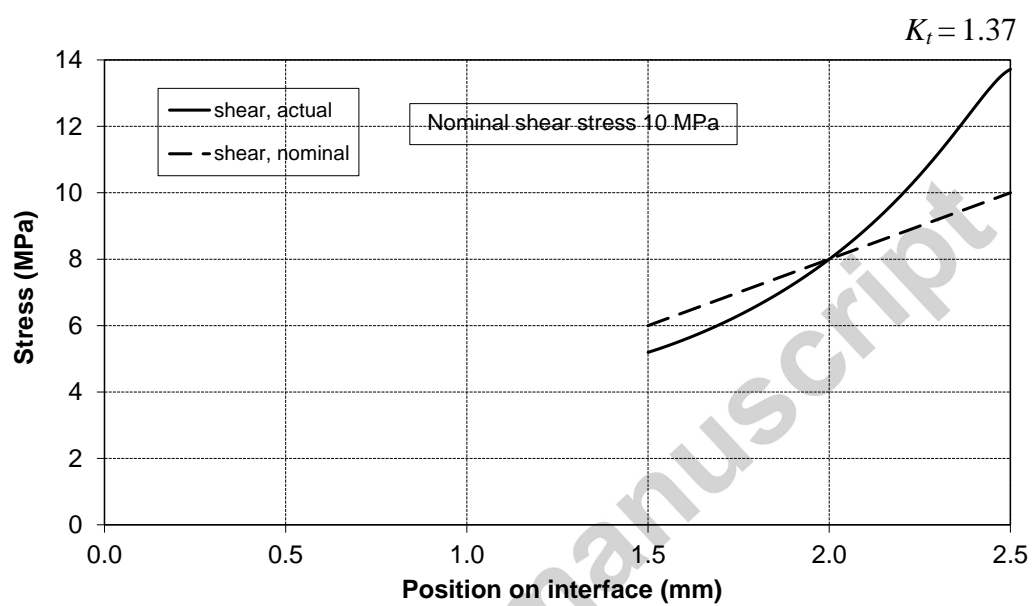


Fig. 7. FE results for the hollow hourglass specimen under torsion: shear stress in the mid-thickness plane of the CA.

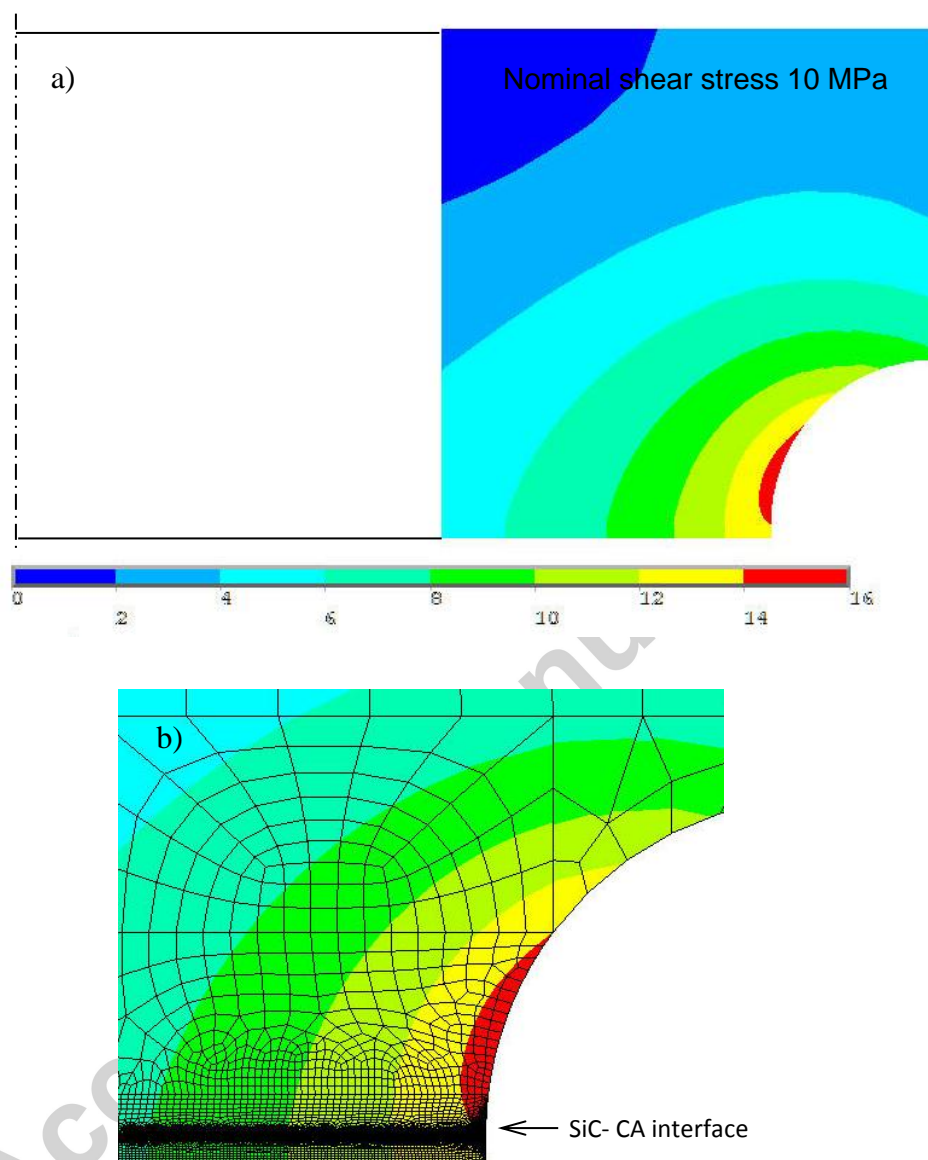


Fig. 8. Contour plot of the major principal stress (MPa) in the hollow hourglass specimen under torsion: a) overall view; b) detail of the stress concentration.

Table 1. Shear strength (mean  $\pm$  standard deviation) obtained from different tests on hourglass specimens by applying eq. (1); selected values from [16].

Specimen type	No. of specimens tested	Fracture in the CA only		Fracture in the CA and SiC	
		Shear strength (MPa)	No. of specimens	Shear strength (MPa)	No. of specimens
Full D=5	12	104 $\pm$ 20	5	113 $\pm$ 21	7
Full D=4	4	103 $\pm$ 12	2	124 $\pm$ 12	2
Hollow (drilled) D=5, d=3	10	-	0	78 $\pm$ 15	10
Hollow (ring) D=5, d=3	17	40 $\pm$ 6	8	89 $\pm$ 21	9

D outside bond diameter, d inside bond diameter (mm).

Table 2. Data relevant to interface singularity.

Material	Angle $\gamma$ (°)	Young's modulus E (GPa)	Poisson's ratio $\nu$ (-)
<sup>#</sup> SiC (adherend)	90	466	0.21
<sup>##</sup> CA glass ceramic (adhesive)	90	140	0.25

<sup>#</sup>From product datasheet [20].

<sup>##</sup>Unpublished results, measurements carried out by Politecnico di Torino.